and McCauley [1980] shows extensive faulting on the eastern wall of Zeami; similarities have been noted between Zeami and certain "floor-fractured" craters on the moon [*Schultz*, 1977; *Head et al.*, 1981]. It seems likely that the interior of Zeami has been influenced by the underlying topography of the area and that a large escarpment or steep slope was present before the event that excavated Zeami. It is possible that the Zeami escarpment/slope may be an extension of the system of faults and lineaments which trend NE of Tolstoj Basin [*Schaber and McCauley*, 1980]. Given the proximity of Zeami to the Mena-Theophanes Basin (see section 4), however, basin rim structure must be considered a possible contributing or alternative explanation for the Zeami escarpment.

7. Equatorial Global Topography

To illustrate the equatorial topography on the global scale, we have plotted all of the composite radar profiles from 1978–1982 on a 0–360° longitude scale in Figure 12. The altitude scale is absolute; the zero-altitude datum is defined by the 2439.0-km-radius reference sphere (see section 2). Figure 13 shows a histogram giving the distribution of altitudes from Figure 12.

The mean of the altitudes in Figure 12 is +0.7 km (2439.7 km mean radius), which is consistent with the 2439 ± 1 km mean equatorial radius measured by *Ash et al.* [1971] from planetary radar observations. Also, there is good spot agreement with the 2439.5 ± 1 km radius measured at 295.3°W, 1.1°N from radio occultations [*Fjeldbo et al.*, 1976]. The zero-altitude datum corresponds to the typical elevation of Mercurian lowlands (see Figure 12 and Figures 2*a*–2*e*) and is close to the "most probable" altitude (+0.3 km) as given by the peak of the histogram (Figure 13).

The extreme range of Mercurian altitudes is 7 km (Figures 12 and 13) as measured from the lowest crater floors to the high plateau near the Mariner 10 eastern terminator. The elevation difference between Mercurian highlands and lowlands is typically about 3 km, which corresponds to the approximate equivalent width of the altitude distribution in Figure 13. For comparison, the moon has approximately 10 km of peak-to-peak relief as measured by Apollo laser altimetry [*Kaula et al.*, 1974]. Some of this relief is due to the roughly 2.5 km offset between the moon's center-of-mass and center-of-figure, since the topographic datum used by *Kaula et al.* [1974] was based on a sphere about the center-of-mass. Altimetry results from the Lunar Sounder Experiment show about 7 km of relief if crater floors are excluded and if the topographic datum is based on a 1738 km sphere about the center-of-figure [*Brown et al.*, 1974].

Radar altimetry for Mercury shows two major topographic highs in the equatorial zone of the planet. The first extends across the eastern terminator in Mariner 10 images from 350°W to 35°W and resembles a plateau with an abrupt drop-off on its western side. This drop in elevation is associated with an extensive system of faults (see section 6). The second major high area covers a broad region south of Caloris Basin between 160°W and 240°W. Caloris itself is approximately bisected by the Mariner 10 western terminator at 190°W longitude. This high area contains two local topographic lows centered on 180°W and 210°W which correspond to areas of smooth plains. A third, less extensive highlands area can be seen in the more northerly profiles near 310°W in the unimaged hemisphere (Figures 2*e* and 12).

The fact that Mercury is in a precise 3:2 spin-orbit resonance indicates that the long axis of the planet's dynamical figure is aligned with the perihelion subsolar points at 0°W

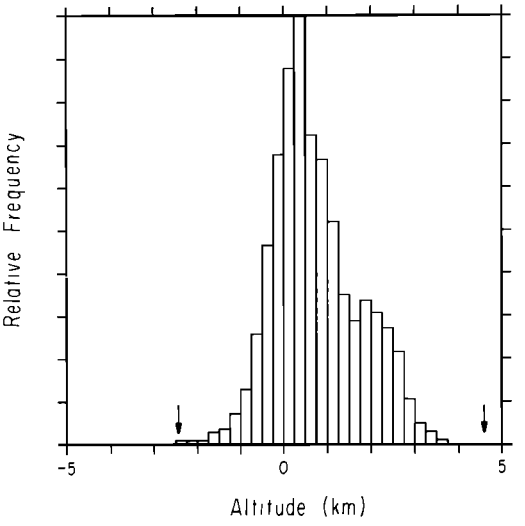

Fig. 13. Histogram of the Mercurian altitudes shown in Figure 12. The histogram is normalized by the number of altitude data points within each altitude bin, not by area. The zero-altitude datum corresponds to a 2439.0-km-radius reference sphere. The highest and lowest altitudes measured are indicated by arrows.

and 180°W longitude. The Arecibo results (Figure 12) show that Mercury's topographic figure is roughly aligned with its dynamical figure, although the two large bulges appear to align somewhat better along a 10°–190°W longitude axis. *Goldreich and Peale* [1966] have shown that a difference between the equatorial moments-of-inertia of only about 0.01% for an ellipsoidal figure would likely ensure a high probability of capture into the 3:2 resonance state. This corresponds to variations in an ellipsoidal dynamical figure of about 100 m. It is then conceivable that the dynamical figure of Mercury could be dominated by a long-wavelength component of uncompensated topography associated with the observed bulges.

An alternative explantion for the 3:2 spin-orbit resonance is that there is a lunar-like mascon associated with the smooth plains in or around Caloris. An early suggestion was made by *Murray et al.* [1974] that the mascon was located in the interior plains of Caloris itself. This was later challenged [*Dzurisin*, 1976; *Melosh and Dzurisin*, 1978*a*] on the basis that a mascon is inconsistent with evidence that the final episode in the tectonic history of Caloris was uplift of the basin floor. *Strom* [1979] points out, however, that this argument against a Caloris mascon presumes that the final uplift was isostatic. *Melosh and Dzurisin* [1978*a*], offering an alternative to a Caloris mascon, argued that a positive gravity anomaly associated with 400 m of uncompensated material in a 1300-km-wide circum-Caloris smooth plains annulus would suffice to control the planet's dynamical figure. *McKinnon* [1979] claims that such an annular ring-load would be "substantially compensated" due to its large size, but that some stresses would be set up which would inhibit complete compensation. The apparent similarity between the circum-Caloris smooth plains and lunar maria, strengthened somewhat by the radar evidence for subsidence, establishes a circum-Caloris mascon as a plausible hypothesis. However, the available data (radar and imaging) are insufficient to determine how much of the smooth plains material remains uncompensated.

8. Conclusions

The Arecibo radar observations of Mercury provide information on the morphology of surface features with horizontal dimensions ranging from the 50 km scales characteristic of